THE TRANSMITTED RADIATION INTENSITY THROUGH A SCATTER

N. Meriç
Ankara Univercity, Faculty of Engineering, Department of Physics Engineering, 06100, Beshevler-Ankara, Turkey

ABSTRACT

Monte Carlo simulation was applied to the investigation of transmitted radiation intensity through a scatterer. Simulations consisted of a pencil beam of monoenergetic photons with energies from 50 keV to 10 meV incident on water, aluminium, iron, copper, tin and lead slabs. We determined the scattered radiation and the scatter fractions recorded in the detector plane. An empirical formula which is a function of the physical parameters scatterer thickness, the linear attenuation coefficient, and the atomic number was obtained for transmitted radiation intensity through a scatterer.

1. INTRODUCTION

In the transmission radiography, the x-rays reaching the detector plane consist of unscattered (primary) and scattered components. While the primary fluence contributes to the signal in the resulting image, the scattered fluence can reduce the contrast and introduce an additional noise. In order to estimate the influence of the scattered radiation on the image quality, the physical characteristics of the scattered radiation must be known.

As x-rays traverse in medium they may be absorbed, pass through without interaction (primary photons), or be scattered. The number of primary photons N_p that strike a detector after passing through a scatterer of thickness L is given by

$$N_P = N_0 e^{-\mu L} \tag{1}$$

Where μ is the linear attenuation coefficient for scatterer at energy E and N_0 is the number of the incident photons. This equation is valid only if the attenuation coefficient is actually a constant which is true only if all of the photons in the incident beam have the same energy (a monoenergetic beam) and the beam is narrow. Some photons may be scattered by the scatterer so that they reach the detector, with the result that the number of the transmitted photons will appear to be larger than primary photons. This situation is usually accounted for replacing Eq. (1) by the following equation

$$N_T = N_0 e^{-\mu L} K(L, E) \tag{2}$$

Where K(L,E) is a rather complicated factor, which is sometimes called a photon buildup factor [1,2] that takes into account the photons scattered by scatterer. The symbols E and L in parentheses indicate the dependence of factor K(L,E) on thickness and energy, respectively.

Intensity of the scattered radiation is an important parameter in designing techniques to reduce the detrimental effects of a scatter on image quality. Clearly, experimental measurements of scatter are very important, but it is very difficult to carry them out. The contribution of the scattered radiation to the image quality has been estimated by many investigators [3-5] using the scatter fraction (F) defined as

$$F = \frac{N_S}{N_T} \tag{3}$$

where N_T is the total number of (scattered and primary) photons that strike the detector and N_S is the scattered component of N_T defined as

$$N_S = N_T - N_P \tag{4}$$

Theoretical investigation of the properties of scattered radiation has been attempted and it has been proven that Monte Carlo (MC) calculation is the most successful method for the simulation of x-ray diffusion in a scattering medium [6-11]. The experimental verifications of the MC method have been demonstrated by several investigators [4-5,12-13].

In this study, we used MC calculations to obtain empirical formula for the total number of photons, N_T, the scattered photons, N_S and scatter fraction, F for different scatterers at the detector plane. The details of our own code and its validity have been described in [12-15]. The resultant equation is a function of three physical parameters; scatterer thickness, linear attenuation coefficient, and atomic number of the scatterer. The results of the formula are compared with the results generated by Monte Carlo simulations and previous x-ray scatter computations.

2. MATERIALS AND METHODS

Figure 1 illustrates the geometry used in the Monte Carlo calculations. A pencil beam of photons enters at the top surface of the scattering material, and the photons are transported through the scattering material. Photons arriving at the bottom surface of the scattering material are absorbed and detected by the detector plane (100% detection efficiency).

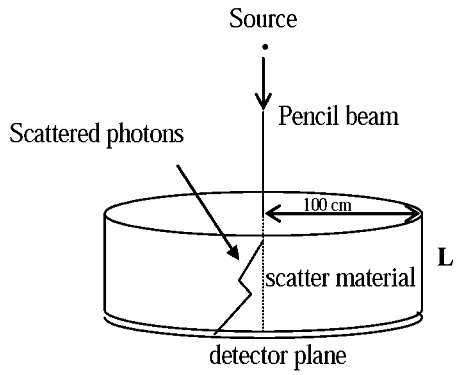

Fig. 1. The geometry used for Monte Carlo simulation of x-ray scattering.

In the calculations, four interaction processes of photons were considered; photoelectric effect, coherent scattering, Compton interaction and pair production. If the interaction was a photoelectric event, photoelectron was traced until it was either escaped from the scatterer or absorbed in the scatterer. Similarly, bremsstrahlung photon and the fluorescence yield were taken into account by tracing the fluorescence photon [16]. If the interaction was a coherent scattering where no energy deposition takes place, the angle of deflection of the photon was found by sampling the Thomson differential cross section corrected for the relativistic atomic form factor [17]. If it was a Compton interaction, the scattering angle was sampled by the Klein-Nishina differential cross section corrected for the electron binding energy [18]. The scattered photon, Compton electron, and Bremsstrahlung photon were traced until they were either absorbed in the scatterer or escaped from the scatterer. If, in the case of pair production, the electron and the positron as well as two annihilation photons were traced accordingly. When the photon was scattered out of the scatterer or when its energy decreased to less than 5 KeV its history was assumed to end. The computations have been carried out by obtaining the linear attenuation coefficients of the scatterer material for the four interaction processes from the data in Storm and Israel [19]. Form factors and scattering functions used in the coherent and incoherent differential cross sections respectively have been calculated by the method given by Johns & Yaffe [20] and Cheng et. al. [21]. Ten runs each having 10^6 photons were used in each iteration.

An PC with a Pentium III coprocessor and 256 MB of RAM was used in this study. All code was written in the computer programming language "C" to run on the PC.

It is well known that N_T depends on the beam energy and scatter thickness. In the first step of our experiments, we used monoenergetic incident x rays to study the energy-dependent behaviour of the scattered radiation. For thin scatterer, the incident photon energy was varied from 50 keV to 1 MeV. For thick scatterer, the incident energy was increased from 1 MeV to 10 MeV. The dimensions of the scatterer and detector were set at 200 cm in diameter. In the second step, the calculations were made using six different scatterer (water, aluminium, iron, copper, tin, and lead) to obtain the dependence of N_T on the atomic number of scatterer. In order to obtain the results in comparable scales, smaller scatterer thicknesses are used for larger atomic number scatterers compared to that of smaller atomic number scatterers. For all measurements, the distance from the source to the input surface of scatter was fixed at 100 cm. All output data, recorded on the detector, included: total number of scattered and primary photons.

The equation below is used to compare our numerical values with the values already exist in literature. Our numerical values are obtained using two different procedures. These are the Monte Carlo techniques and the equation, which we obtained from our numerical results.

$$\Psi = \left\{ \frac{1}{n} \sum_{i=1}^{n} \left(\frac{F(\text{MC or Eq.})}{F(\text{Lit.})} - 1 \right)_i^2 \right\}^{1/2} \tag{5}$$

Where F(Lit.), F(MC), and F(Eq.) are the values taken from the literature, calculated with our Monte Carlo calculation and obtained equation, respectively. F(MC or Eq.) means either F(MC) or F(Eq.). n means the number of data points.

3. RESULTS AND DISCUSSION

Photons striking the detector after passing through a scatterer of thickness L is scored according to scattered and primary photons categories for a variety of scatterer thicknesses (0.1 mm – 200 cm), incident photon x-ray energies (50 keV -10 MeV) and different atomic number of scatterer (water, aluminium, iron, copper, tin and lead). The results of the Monte Carlo calculations are presented in the form of total number of (scattered and primary) photons, N_T, the scattered photons, N_S and scatter fraction, F.

3.1. TOTAL NUMBER OF PHOTONS ON THE DETECTOR

A curve could be fitted to the obtained by the above mentioned way for the total number of photons, N_T, at the detector data using the method of least squares and the equation of the curve was determined as follows:

$$N_T = \left[N_0 e^{-\mu L} \right] \left[\sqrt[3]{\left(1 + \frac{1}{2}\mu L\right)^4} \exp\left[\left(\frac{1}{8} - \frac{Z}{300}\right)\mu L \right] \right] \tag{6}$$

Where Z is the atomic number of the scatterer. The expression in the first square bracket in Eq.(6) represents the attenuated primary beam. The term in the second square bracket is the photon build up factor that takes into account the photons scattered by scatterer. Note that K(E,L), at the same time, is a function of Z. The fit based on Eq.(6) is compared with the data obtained from MC results and it is shown in Figure 2. The total number of photons is normalized to 100 incident photons. In these figures, the functional dependency of N_T on energy, thickness, and the atomic number of the scatterer are shown. Each curve in these figures represents a different scatterer. An excellent agreement between the MC and Eq. (6) appears in these figures.

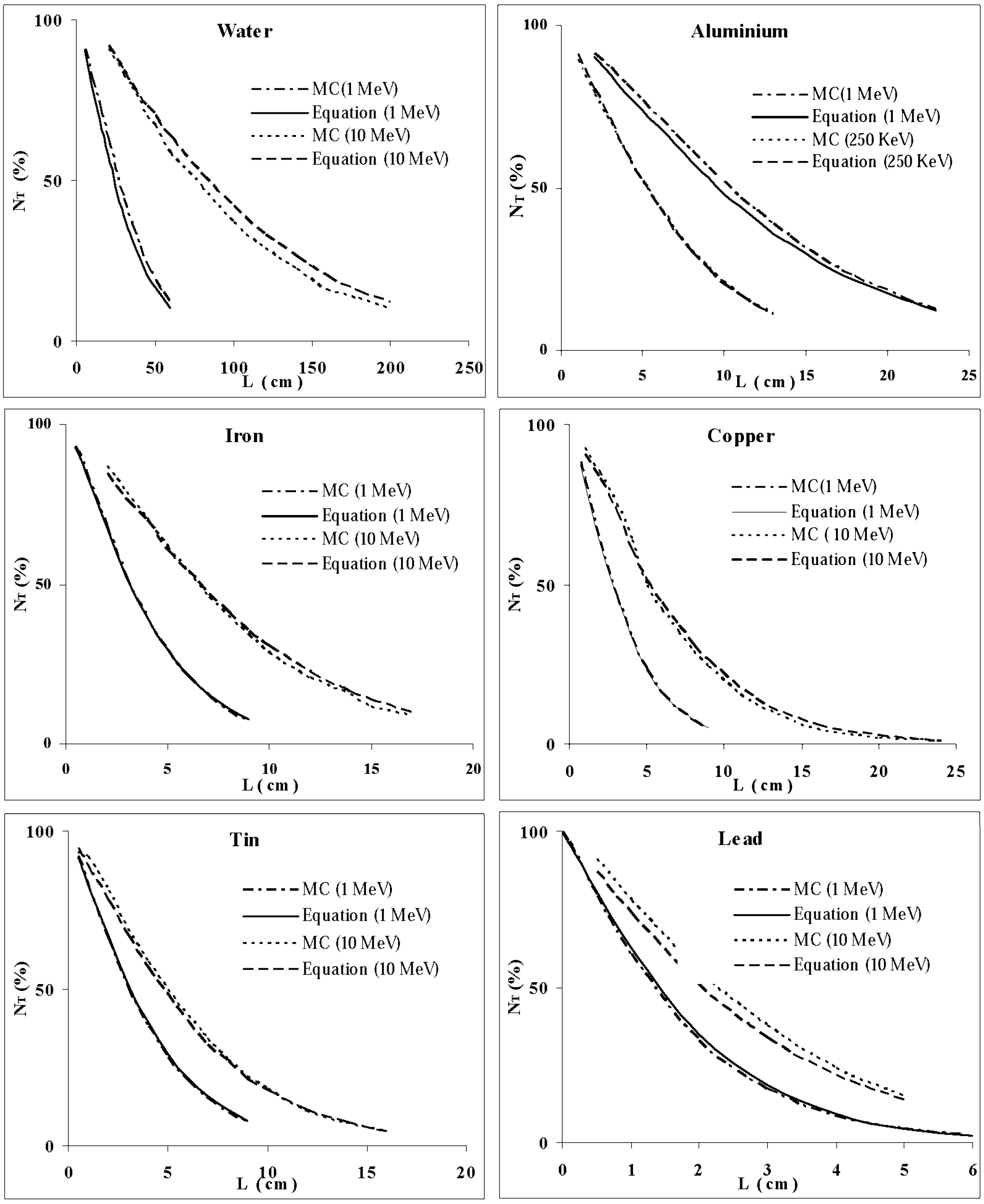

Fig. 2. Calculated number of the detected photons (N_T) and fits based on Eq. (6) for different materials, thicknesses and energies. MC : Monte Carlo calculations.

As shown in these figures, for thin scatterer, more primary photons are scattered than that of transmitted photons. However, as the scatterer thickness increases, the scattered photons become the dominant component. The ratio of the number of scattered photons to the number of primary photons increases with increasing incident energy. Nevertheless, photons are absorbed in the scatterer. For a given energy, the number of absorbed photons increase as the scatterer thickness increases. The increase can be attributed to an increase in multiple scattering of photons in thicker scatterer. Therefore, the total numbers of photons decrease as the thickness increases.

3.2. SCATTERED PHOTONS ON THE DETECTOR

The empirical formula we obtained by the above mentioned way for total number of scattered photons, N_s at the detector is

$$N_S = \left[N_0 e^{-\mu L} \right] \left(\left[\sqrt[3]{(1+\frac{1}{2}\mu L)^4} \exp\left[(\frac{1}{8} - \frac{Z}{300})\mu L \right] \right] - 1 \right) \tag{7}$$

The numerical results obtained from Eq.(7) are plotted together with MC results in Figure 3. The number of scattered photons is normalized to 100 incident photons. Figure 3 shows the scattered photons reaching the detector plane as a function of monoenergetic incident photon energy irradiating the scatterer. The number of these scattered photons increases to a maximum and then decreases monotonically as the thickness increases.

3.3. SCATTER FRACTION

If Eq.(6) and (7) are substituted into Eq.(3), scatter fraction, F at the detector can be written as follows

$$F = 1 - \frac{\exp\left[-(\frac{1}{8} - \frac{Z}{300})\mu L \right]}{\sqrt[3]{(1+\frac{1}{2}\mu L)^4}} \tag{8}$$

The numerical results obtained from Eq.(8) are plotted together with MC results in Figure 4. As can be seen from this figure, the scatter fraction increases rapidly as the thickness of the scattering medium increases.

3. 4. COMPARISON WITH PREVIOUS WORKS

Scatter fractions have been determined experimentally for lucite, polyethylene, aluminium and copper of varying thicknesses using a x-ray beam of 67 kVp (H = 0 cm air gap, W = 2 cm beam diameter, A = 10x10 cm^2 scatter dimensions) by Meric et al. [13]. The mean energies of the 67 kVp incident spectra in this study were calculated as 52 keV. In order to compare our scatter fraction results with the data from this reference we used the mean photon energy of x-ray beam (52 keV). The results are shown in Figure-5. As seen from this figure our scatter fraction results are slightly higher than those reported by Meric et al. This is attributed to the larger scatter and detector dimensions used in our studies.

In order to check the validity of Eq. (8), the scatter fractions obtained using this formula and our Monte Carlo calculations for water and aluminium are given in Tables 1 and 2 together with Papin and Riely's [22] calculation. In their calculation they used a very large water and aluminium scatter material (200x200xL cm^3), monoenergetic pencil beams in the energy range of 70-110 keV, and a very large surface detector (200x200 cm^2) at the exit plane of the scatter. The mean relative deviation given by Eq. (5) was used for the comparison of our results with Papin and Rielly's result and presented in table 3. As seen from Tables 3, the relatively small differences between the results (10% in the worst case) may also be attributed to statistic fluctuations or to systematic errors in the input data as discussed in Barnea and Dick [3].

It is difficult to compare our results with the previously published data because scatter is highly dependent on geometric considerations. A comparison can be made with Eq. (8), which is the one obtained from Jaffray et al [23], using their plots of scatter fraction (F) against the product of the radial position for poly-methyl-methacrylate (which has an infinite lateral extent). Our F value is 0.28 at 6 MeV for L=17 cm whereas the corresponding value derived from Jaffray's plots for 5x5 cm^2 field size and 0 cm air gap is 0.26.

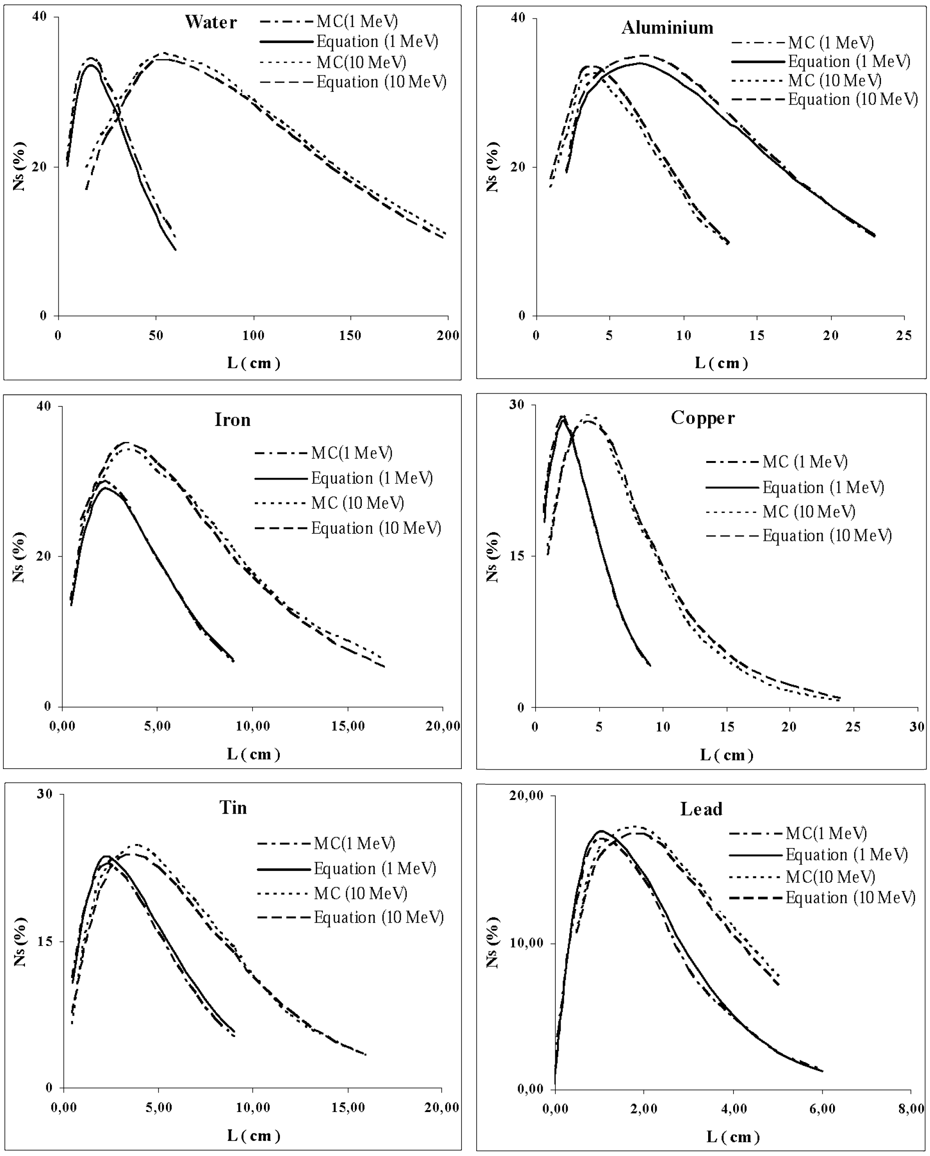

Fig. 3. Calculated number of the scattered photons detected (N_s) and fits based on Eq. (7) for different materials, thicknesses and energies. MC : Monte Carlo calculations.

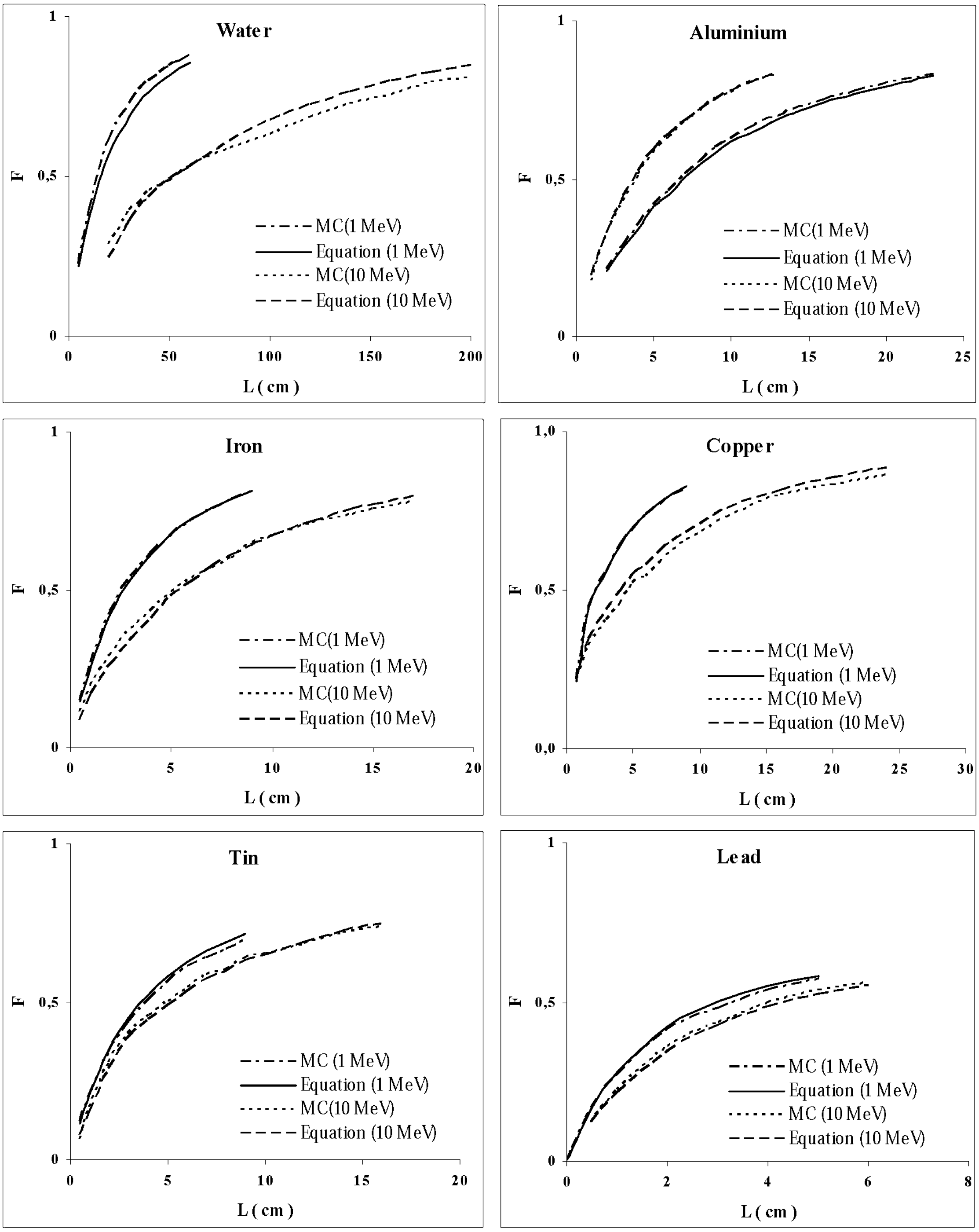

Fig. 4. Calculated scatter fraction (F) for the photons detected and fits based on Eq. (8) for different materials, thicknesses and energies. MC: Monte Carlo calculations.

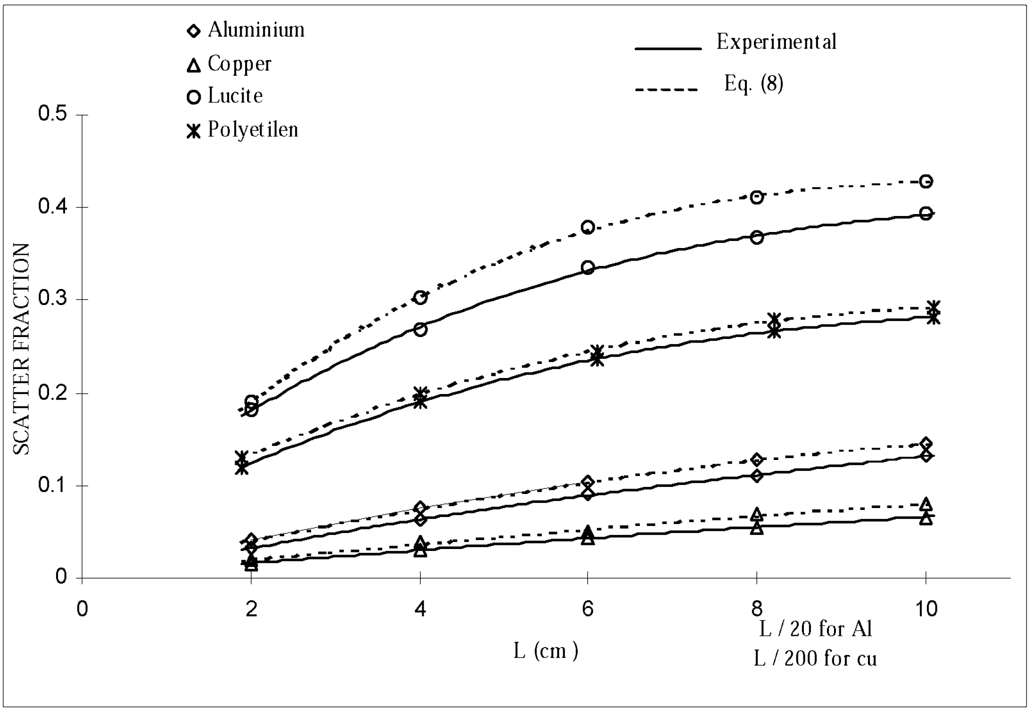

Fig. 5 - Variation of the measured and obtained from Eq(8) scatter fractions; for different thicknesses (L) and various materials.

Table 1. Comparison of scatter fractions for water as a function of thickness.

L(cm)	70 keV			90 KeV			110 KeV		
	Papin-Rielly	Eq.(8)	MC	Papin-Rielly	Eq.(8)	MC	Papin-Rielly	Eq.(8)	MC
0.5	0.057	0.052	0.070	0.055	0.050	0.064	0.054	0.048	0.060
1.0	0.109	0.103	0.133	0.107	0.098	0.122	0.105	0.094	0.116
2.0	0.207	0.193	0.240	0.204	0.185	0.223	0.202	0.178	0.212
3.0	0.292	0.276	0.329	0.287	0.264	0.307	0.283	0.257	0.293
4.0	0.371	0.342	0.402	0.364	0.336	0.377	0.358	0.328	0.362
5.0	0.436	0.407	0.464	0.431	0.400	0.438	0.425	0.396	0.421
6.0	0.492	0.464	0.517	0.488	0.458	0.490	0.484	0.446	0.472
7.0	0.540	0.513	0.562	0.539	0.508	0.535	0.538	0.503	0.517
8.0	0.581	0.552	0.602	0.584	0.547	0.574	0.579	0.546	0.556
9.0	0.624	0.587	0.636	0.625	0.588	0.609	0.620	0.584	0.591
12.0	0.717	0.680	0.717	0.719	0.681	0.691	0.717	0.679	0.674
15.0	0.779	0.746	0.774	0.786	0.748	0.751	0.789	0.748	0.735

Table 2. Comparison of scatter fractions for aluminum as a function of thickness.

L(cm)	70 keV			90 KeV			110 KeV		
	Papin-Rielly	MC	Eq.(8)	Papin-Rielly	MC	Eq.(8)	Papin-Rielly	MC	Eq.(8)
0.18	0.049	0.048	0.063	0.048	0.046	0.050	0.047	0.044	0.045
0.37	0.094	0.094	0.122	0.092	0.090	0.098	0.091	0.084	0.088
0.74	0.173	0.171	0.217	0.173	0.166	0.178	0.171	0.159	0.161
1.11	0.239	0.240	0.294	0.241	0.233	0.245	0.241	0.228	0.223
1.48	0.293	0.296	0.356	0.298	0.293	0.302	0.304	0.288	0.277
1.85	0.344	0.344	0.408	0.354	0.342	0.351	0.357	0.340	0.323
2.22	0.385	0.387	0.452	0.401	0.382	0.393	0.404	0.384	0.364
2.59	0.426	0.427	0.489	0.435	0.425	0.429	0.446	0.424	0.399
2.96	0.453	0.465	0.521	0.472	0.458	0.461	0.482	0.460	0.431
3.33	0.488	0.492	0.548	0.503	0.490	0.489	0.516	0.493	0.459
4.44	0.573	0.566	0.613	0.588	0.568	0.557	0.595	0.579	0.528
5.55	0.637	0.630	0.658	0.649	0.630	0.607	0.656	0.637	0.580

Table 3. Comparison with Papin and Rielly's result using ψ values.

Scatter	70 keV		90 keV		110 keV	
	Eq.(8) vs Papin	M.C. vs papin	Eq.(8) vs Papin	M.C. vs papin	Eq.(8) vs Papin	M.C. vs papin
Water	10.03	7.19	6.79	7.76	5.88	8.88
Aluminum	10.13	1.17	4.43	3.40	10.35	5.66

4. CONCLUSION

The basic motivation for this study was to develop the photon buildup factor, K(L,E), in Eq.(2) for estimating the transmitted radiation intensity which is valid for wide energy and thickness ranges and different scatterer types. The empirical formula we obtained in this study gives results which are in good (max. 10% different) agreement with that of MC results and earlier published data.

The empirical formulas we have obtained for the total number of photons (Eq. (6)) and the scatter fraction (Eq. (8)) are valid for monoenergetic incident x rays. Since each photon interacts independently with the scattering medium, the corresponding results for polyenergetic incident beams can be derived from a weighted sum of the results of their monoenergetic components. The results discussed in this paper can thus be applied to any polyenergetic incident beam.

5.ACKNOWLEDGMENT

This work was supported by the Scientific and Technical Research Council of Turkey (TUBITAK) [TBAG-2032 (101T053)].

6.REFERENCES

1. G. F. Knoll: Radiation detection and measurement. (1979) 1 st ed. John Wiley and Sons Inc 70.
2. H. E. Johns, J. R. Cunningham: The Physics of Radiology. (1983) 4th edn. Charles C. Thomas Publisher Springfield Illinois USA 139.

3. G. Barnea and C.E. Dick: Med. Phys. **13** (1986) 490.

4. C. E. Dick, C. G. Soares, J. W. Motz : Phys. Med. Biol. **23** (1978) 1076 .

5. H. P. Chan and K. Doi: Phys. Med. Biol. **28** (1983) 109.

6. K. Doi, H. P. Chan: Radiology **135** (1980) 199.

7. H. P. Chan, K. Doi : Med. Phys. **11** (1984) 480.

8. H.P. Chan, K. Doi: Med. Phys. **12** (1985) 152.

9. H. P. Chan, K. Doi: Med. Phys. **13** (1986) 824.

10. J. M. Boone, J. A. Seibert: Med. Phys **15** (1988) 713.

11. J. M. Boone, J. A. Seibert: Med. Phys. **15** (1988) 721.

12. N. Meriç, D. Bor, N. Buget, M. Özkırlı: Physica Medica **14** (1998) N1 3.

13. N. Meriç, D. Bor, N. Buget: Applied Radiation and Isotopes **51(2)** (1999) 161.

14. N. Meriç, D. Bor, E. T. Ilgıt, İ. İ. Öznur, N.Büget:Physica Medica **14**(1998)N3 95.

15. N. Meriç: Applied Radiation and Isotopes. **55(4)** (2001) 557.

16. R. L. Morin: Monte Carlo simulation in the radiological sciences CRC press inc (1988) pp. 108 Florida.

17. J. H. Hubbell, I. Overbo: J. Phys. Chem. Ref. Data **8** (1979) 69.

18. J. H. Hubbell, W. J. Veigele, E. A. Briggs, R. T. Brown, D. T. Cromer, R. J. Howerton: J. Phys. Chem. Ref. Data **4** (1975) 471; Erratum: **6** (1977) 615.

19. E. Storm, H. I. Israel: Nuclear Data Tables. **A7** (1970) 565.

20. P. C. Johns, M. J. Yaffe : Med. Phys. **10** (1983) 40.

21. C. W. Cheng, K. W. Taylor, A. F. Holloway: Med. Phys **22** (1995) 1235.

22. P. J. Papin, P. S. Rielly: Med. Phys.**15** (1988) 909.

23. D. A. Jaffray, J. J. Battista, A. Fenster, P. Munro: Med. Phys. **21** (1994) 45.